Light Metals 2011 *Edited by: Stephen J. Lindsay*
TMS (The Minerals, Metals & Materials Society), 2011

Light Metals 2011

ELECTRODE TECHNOLOGY for ALUMINUM PRODUCTION

ORGANIZERS

Alan Tomsett
Rio Tinto Alcan
Brisbane, Australia

Barry Sadler
Net Carbon Consulting Pty. Ltd.
Victoria, Australia

Light Metals 2011 *Edited by: Stephen J. Lindsay*
TMS (The Minerals, Metals & Materials Society), 2011

Light Metals 2011

ELECTRODE TECHNOLOGY for ALUMINUM PRODUCTION

Anode Baking

SESSION CHAIR
Said Al Maawali
Sohar Aluminium
Oman

Light Metals 2011 *Edited by: Stephen J. Lindsay*
TMS (The Minerals, Metals & Materials Society), 2011

Predicting the Response of Aluminum Casting Alloys to Heat Treatment

Chang-Kai Wu, Makhlouf M. Makhlouf
Advanced Casting Research Center
Worcester Polytechnic Institute (WPI); 100 Institute Rd., Worcester, MA 01609, USA

Keywords: Heat treatment, Quenching Factor Analysis, Modeling

Abstract

In this publication we report on the development of a mathematical model that enables predicting the changes in hardness of cast aluminum alloy components in response to heat treatment. This model is part of a more inclusive model that is currently under development and that when completed, will enable predicting the changes in room temperature tensile properties as a function of heat treatment.

The model uses the commercially available finite element analysis software (ABAQUS) and an extensive database that was developed specifically for the aluminum alloy under consideration (namely, A356.2). The database includes mechanical, physical and thermal properties of the alloy all as functions of temperature. In addition, boundary conditions – in the form of the heat transfer coefficient associated with each one of the heat treatment steps – are obtained from measurements performed with specially designed quenching devices. The database and boundary conditions are used in a thermal analysis module and a user-developed module. The user-developed module uses Quench Factor Analysis to predict the maximum attainable hardness that develops in a commercial cast component that is subjected to a standard commercial heat treating cycle. A heat-treated part was used to validate the model prediction.

Introduction and Background

The mechanical properties of aluminum alloy castings can be greatly improved by a precipitation hardening heat treatment. A typical precipitation hardening heat treatment consists of three steps: (1) solutionizing, (2) quenching, and (3) aging; and is performed by first heating the casting to and maintaining it at a temperature that is a few degrees lower than the solidus temperature of the alloy in order to form a single-phase solid solution. Then rapidly quenching the casting in a cold (or warm) fluid in order to form a supersaturated non-equilibrium solid solution; and finally, reheating the casting to the aging temperature where nucleation and growth of the strengthening precipitate(s) can occur.

The objective of this work is to develop a model and the necessary material database that allow predicting these physical and material property changes. The structure of the model is described in Figure 1. A thermal module calculates the thermal history of the part during quenching. The time-temperature output from the thermal module becomes input to a user-developed property module. This is a module and database for predicting the maximum resultant room temperature hardness attainable after aging at each node within the model of the cast component. This is done by a Quench Factor Analysis (QFA) [1].

Quench Factor Analysis was first developed by Evancho and Staley [1] in 1971 to predict the effect of continuous quenching on yield strength and corrosion resistance of wrought aluminum alloys. Since then, the QFA method has proved to be a very useful tool in predicting properties of many cast and wrought aluminum alloys [2]. The QFA method is based on using isothermal precipitation kinetics to predict the results of non-isothermal conditions during continuous cooling. In doing so, it considers the cooling curve to be made up of a series of isothermal transformation steps and adds up the amount of second phase transformed during each of these isothermal steps in order to simulate the overall degree of super saturation of the alloy.

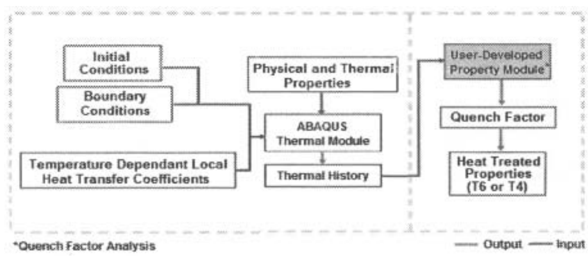

Figure 1. Description of the Model.

Assuming that the precipitation transformation follows the Johnson-Mehl-Avarmi-Kolmogorov (JMAK) equation, for continuous transformations, the term t in the JMAK equation may be replaced by the Quench Factor (Q) [3]. Rometsch [4] suggested that the development of strength in a precipitation hardened metallic component is proportional to the square root of the volume fraction of precipitate, so that maximum value of the achievable strength for an alloy can be described by Eq. (1). In Eq. (1), σ is the predicted peak strength, $\sigma_{\min}$ and $\sigma_{\max}$ are the minimum and maximum values of the strength achievable for the alloy, and K_1 is a constant.

$$\frac{c - c_{\min}}{\sigma_{\max} - \sigma_{\min}} = [\exp(-K_1 Q)]^{\frac{1}{2}} \qquad (1)$$

In order to obtain the cumulative Quench Factor (Q), incremental quench factors (q_f) are calculated for each increment on the cooling curve as the ratio of the time that the material spends at the specific temperature (Δt_i) divided by the critical time that is required for a certain amount of transformation to occur at that temperature(C_{t_i}). The incremental quench factor values are then summed up over the entire transformation temperature range in order to produce the cumulative Quench Factor (Q), as shown in Eq. (2).

$$Q = \sum q_f = \sum_{T_1}^{T_i} \frac{\Delta t_i}{C_{ti}} \qquad (2)$$

In order to use Eq. (2), the cooling path taken by the material during quenching must be known. One way of representing the cooling path is *via* a time-temperature-property (TTP) curve. This curve is often referred to as the 'C' curve of the material. The TTP curve is a graphical representation of the transformation kinetics that influences the material's mechanical properties and defines the time that is required to precipitate sufficient solute to alter the strength of the material by a specified amount. The C curve may be defined mathematically by the critical time function (C_t), which is given by Eq. (3). In Eq. (3), C_t is the critical time required to form a specific quantity of a new phase. K_1 to K_5 are constants that depend on the material [5]. K_1 is equal to the natural logarithm of the fraction of material which is untransformed during quenching, K_2 is related to the reciprocal of the number of nucleation sites, K_3 is related to the energy required to form a nucleus (J/mol K), K_4 is related to the solvus temperature (K), and K_5 is related to the activation energy for diffusion (J/mol), R is the universal gas constant (J/mol K), and T is absolute temperature (K). The main idea of QFA is to transform the TTP curve into a mathematical equation that can be used for calculating the volume fraction of precipitate that form during quenching in terms of loss of strength.

$$C_t = -K_1 \times K_2 \times \exp\left[\frac{K_3 \times (K_4)^2}{RT(K_4 - T)^2}\right] \times \exp\left[\frac{K_5}{RT}\right] \quad (3)$$

Materials and Procedures

Aluminum casting alloy A356.2 is used to develop and demonstrate the procedure for obtaining the necessary database and modeling the response of aluminum alloy cast components to T6 heat treatment. The data includes mechanical properties and heat transfer coefficients for various process steps as functions of temperature. Other required thermal and physical properties, such as density, specific heat, etc., are obtained from JMatPro Software[1]. The methodology developed in modeling A356.2 alloy castings can be easily extrapolated to other Al-Si alloys.

Thermal Conductivity

Needless to say, thermal conductivity is an important parameter required for heat transfer analysis. The thermal conductivity of A356.2 alloy in the as-cast condition was measured at several temperatures according to ASTM standard E1225-04. The measured thermal conductivity was compared to values published in reference [6] and was found to be in good agreement in the temperature range between 100°C (212°F) and 400°C (753°F).

Heat Transfer Coefficients

The quenching heat transfer coefficient (HTC) is used by the thermal module in ABAQUS to compute the heat that is transferred out of the casting during quenching. Measurement of the quenching HTC involves quenching hot cylindrical probes that are machined from cast A356.2 alloy and equipped with a k-type thermocouple that is connected to a data acquisition system, into the quenching medium and acquiring the temperature-time curve [7]. Prior to quenching, the probes are heated to the solutionizing temperature for 12 hours. A heat balance analysis (usually referred to as a lumped parameter analysis) performed on the system (i.e., the probe + the quenching medium) results in Eq. (4), which yields HTC [8]. In Eq. (4), $h(T)$ is the quenching heat transfer coefficient of the probe, ρ, V, C_p, and A_s are the density, volume, specific heat, and surface area of the probe, respectively. T_s is the temperature of the probe and T_f is the bulk temperature of the quenching medium. The derivative of temperature with respect to time $\left(\text{i.e.}, \frac{dT}{dt}\right)$ is calculated from the measured temperature *vs*. time data.

$$h(T) = -\frac{\rho V C_p}{A_s (T_s - T_f)} \frac{dT}{dt} \quad (4)$$

In order to determine the HTC with this method, a cylindrical quenching probe, 0.375 inch (9.53 mm) in diameter and 1.5 inch (38.1 mm) in length, and a quenching disk, 1.1 inch (27.94 mm) in diameter and 0.3 inch (7.62 mm) in thickness, were cast and machined from standard A356.2 alloy. Thermocouples were placed in the molds at the geometric center of each casting. During measurements, both the cylinder and disk were quenched from 538°C (1000°F) into three different quenching media: (i) hot water that is maintained at 80°C (176°F), (ii) static room temperature air, and (iii) forced-air obtained by an industrial fan. Figure 2 shows the measured heat transfer coefficients by quenching probe and disk into hot water as a function of temperature. HTC for quenching in static room temperature air ranged between 14~41 W/m^2, and that for quenching in forced-air ranged between 168~181 W/m^2.

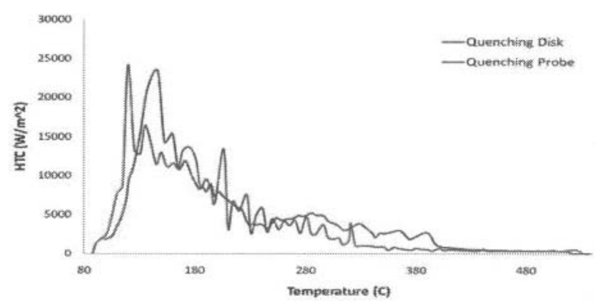

Figure 2. Quenching heat transfer coefficient measured for 80°C (176°F) hot water.

Temperature-Dependant Local Heat Transfer Coefficients

For decades, many researchers have tried to determine heat transfer coefficients for various processes analytically [9] and many have tried to determine it experimentally [10]. However, heat transfer coefficients are very much dependant on part geometry, quenching medium and quenching process and this makes their determination difficult and the values obtained are approximate at best. More recently, a computer program has been developed for determining heat transfer coefficients in casting and quenching processes [11]. However, quenching a hot object into a fluid involves complex thermodynamic, fluid dynamic and phase transformation interactions that occur simultaneously and make the necessary simulations require a long time even with the fastest computer processor. For these reasons, an efficient method for obtaining quenching heat transfer coefficients for simulation purposes is needed.

[1] Developed and marketed by Sente Software Ltd., Surrey Technology Centre, 40 Occam Road, GU2 7YG, United Kingdom.

Before discussing our effort towards this end, it is necessary to briefly review what happens during quenching. There are three distinct stages during quenching. These are: (1) formation of a vapor blanket around the solid part, (2) nucleate boiling of the quenching medium, and (3) convective cooling of the solid part. Each of these three stages is associated with a distinct cooling regime and heat transfer from the solid surface is very much dependant on small variations in the conditions of the quenching bath and the state of the metal surface. Particularly, the formation of the vapor blanket around the solid surface creates a problem in modeling the quenching process: Due to the large difference between the thermal conductivity of air and that of water, contact of the solid surface with air bubbles decreases the cooling rate while its contact with cold water increases it.

In a typical casting, some features may trap the vapor phase and other features may restrict the movement of the quenching fluid causing the fluid in contact with these areas to heat up locally. These effects can reduce the local cooling profile. In this work, an assumption has been made that the air entrapments or restricted air flow can be represented by assigning different heat transfer coefficients in local regions. In order to verify the validity of this assumption, five simple shapes were considered. These shapes allow representation of almost all of the features that may be present in a typical casting. Once the heat transfer coefficient for each one of these shapes is determined, it may be applied locally to the corresponding feature on a complex casting that is to be simulated. There are two important advantages in locally applying the quenching heat transfer coefficients in computer simulations. These are: (1) the boundary conditions for the model become more representative of the physical situation, and (2) the computational time is significantly reduced. The five selected geometric shapes are shown schematically in Figure 3 and they are as follows:

1. A free surface over which bubbles and/or vapor that is produced during quenching can escape freely into the surrounding fluid.
2. A cavity where bubbles and/or vapor that is produced during quenching are trapped and form an air pocket.
3. A channel where water flow is restricted and so the water temperature is locally higher than the average bath temperature.
4. A horizontal surface against which the vapor phase that is produced during quenching is trapped giving rise to a smaller heat transfer coefficient.
5. An angled surface that affects the rise of the vapor phase that is produced during quenching through the quenching fluid thus decreasing the magnitude of the heat transfer coefficient (the magnitude of the heat transfer coefficient in this case may be different from that in case 4).

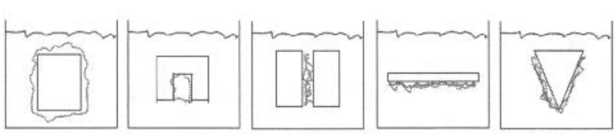

Figure 3. Five shapes used for determining the quenching heat transfer coefficients. The red lines represent vapor and/or gas bubbles.

These shapes were cast and instrumented with thermocouples. Some castings were machined so as to create the necessary features. The castings were solutionized at 538°C (1000°F) and then quenched into water that is maintained at 80°C (176°F). A thermal module was made for each of the geometries and the exact quenching conditions were used to simulate each part. In calculating the temperature changes during quenching, each surface was assigned one of the measured quenching heat transfer coefficients that were measured either by quenching probe or disk in contact with water or air, depending on the local quenching conditions. For example: in case (2), it is assumed that the cavity volume is completely filled with air from the start of the quenching event until its end, so the cavity surfaces were assigned the measured heat transfer coefficient for static air. The remaining surfaces were assigned the measured hot water heat transfer coefficient obtained by the quenching probe. In case (4), the flat bottom surface was assigned the measured hot water heat transfer coefficient from the quenching disk and the remaining surfaces were assigned the measured hot water heat transfer coefficient from the quenching probe.

Each of the five castings was quenched and the cooling rate *vs.* temperature was recorded and compared to the computer-calculated cooling rate *vs.* temperature. In all cases, there is excellent agreement between the measured and computer-calculated curves indicating that the developed temperature-dependent local heat transfer coefficients can be used for thermal simulations on different shape castings. The procedure described above provides a useful means of resolving the issues caused by the vapor blanket and air pockets that form unevenly in and around typical castings and cause uneven cooling that results in different cooling profiles from location to location on the same casting. However, details in commercial castings are usually very complicated and it may not be easy to manually assign a heat transfer coefficient to each and every surface on such complex castings. However, a computer module may be easily developed to accomplish this task.

Kinetics Parameters for Quench Factors Analysis

The aging curve for A356.2 alloy was needed in order to perform the Quench Factor Analysis. The aging curve was obtained by measuring the Rockwell hardness B scale (HRB) of the alloy. The HRB measurements were performed with a steel ball indenter that is 1/16 inch (1.59 mm) in diameter and a minor and major load that are 98N and 883N, respectively. The result is shown in Fig. 4. In order to obtain this data, small identical samples of A356.2 alloy were solutionized at 538°C (1000°F) and then quenched into ice water. These samples represent the maximum possible quenching rate. Subsequently, the samples were aged at 155°C (311°F) for different periods of time and their hardness was measured. The values were averaged from 20 to 40 measurements and the maximum value was found to be 65 HRB. It was achieved after aging for 19 hours. This number represents the maximum hardness value in the Eq. (1); i.e., σ_{max}. The value for the minimum hardness in Eq. (1); i.e., σ_{min}, was obtained by furnace cooling the samples after solutionizing. The cooling rate in the furnace was found to be less than 0.2°C/s, and σ_{min} was found to be 8 HRB.

Next, the Jominy End Quench test described in ASTM-A255 was used to determine the kinetics parameters. A356.2 alloy Jominy End Quench bars that are 1 inch (25.4 mm) in diameter and 4 inches (101.6 mm) long were cast in a permanent mold. The bars were then instrumented with thermocouples at seven different locations along their length in order to record the local cooling data during the end quenching process. The thermocouples were evenly distributed at 0.5 inch (12.7 mm) increments along the length of the bar. The bar was solutionized for 12 hours at 538°C (1000°F) and then quenched from one end by cold tap water while the time-temperature data was being recorded. The unidirectional heat transfer thus created results in a progressively decreasing cooling rate along the length of the bar. The recorded cooling curves and cooling rates *vs*. temperature are presented in Figure 5Figure 6, respectively.

Small flat surfaces were then made along the length of each quenched bar by rubbing the surface with fine sand paper in order to allow for accurate hardness measurement on the flat surface of the bar. HRB measurements were then performed around the perimeter at the thermocouple locations. Because the measured HRB is an arbitrary number with no physical meaning, the HRB values were converted into Meyer hardness [12] for the purpose of calculation and then they were converted back to HRB for presentation.

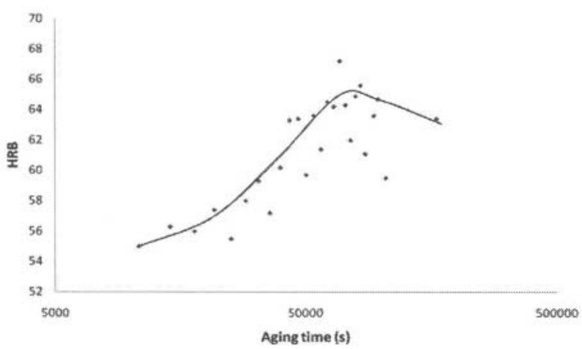

Figure 4. Measured HRB *vs*. aging time for A356.2 aluminum alloy.

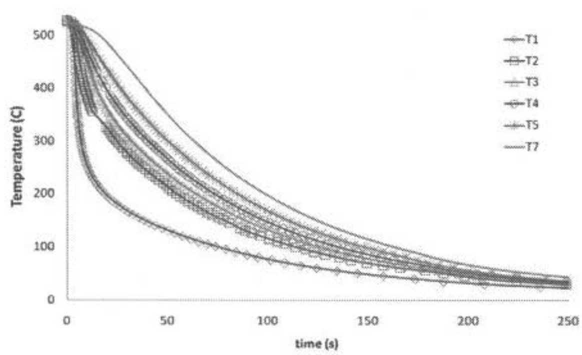

Figure 5. Recorded cooling curves at different locations along the length of the A356.2 aluminum alloy Jominy End Quench bar.

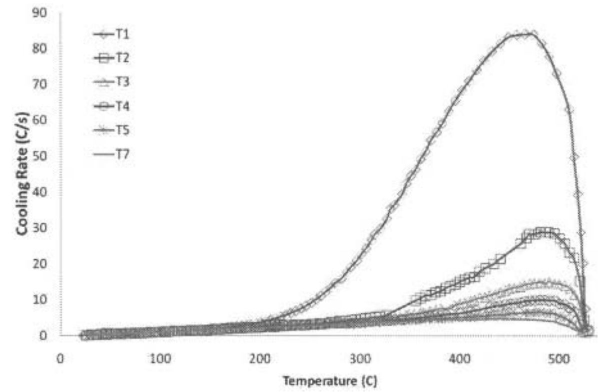

Figure 6. Recorded cooling rates for different locations along the length of the A356.2 aluminum alloy Jominy End Quench bar.

In order to determine the kinetics parameters K_1, K_2, K_3, K_4, and K_5 that appear in the C_t function described by Eq. (3), previous researchers [1, 2, 3, 4, 5, and 13] used mathematical equations or other analytical methods which vary the five unknown constants simultaneously in Eq. (3) in order to fit the experimental data. This is a difficult task since different combinations of the five constants could yield equally good fits of the experimental data [14]. In this work, a new approach was adopted wherein three out of the five unknown kinetics parameters; namely, K_1, K_4, and K_5, were fixed, and only K_2 and K_3 were made to vary. K_1 is easily found since it is the natural log of the fraction of material that is untransformed during quenching. K_4 and K_5 are the solvus temperature of A356.2 and the activation energy for aging the precipitates [17], respectively.

Eq. (1) may be re-written as follows,

$$Q = 2\ln\left(\frac{\sigma - \sigma_{\min}}{\sigma_{\max} - \sigma_{\min}}\right) \times \frac{-1}{K_1} \tag{5}$$

According to Eq. (5), the Quench Factor (Q) may be determined from the measured hardness values (σ, σ_{max} and σ_{min}) and K_1. Also, the Quench Factor (Q) may be determined from the local cooling data and the C_t function. The C_t function is given by Eq. (3), which can be re-written as follows,

$$Q = \sum_{T_1}^{T_i}\left[\frac{\Delta t_i}{\left(-K_1 \times K_2 \times \exp\left[\frac{K_3 \times (K_4)^2}{RT(K_4 - T_i)^2}\right] \times \exp\left[\frac{K_5}{RT_i}\right]\right)}\right] \tag{6}$$

The Quench Factor (Q) calculated from Eq. (5) was plotted against the Quench Factor calculated from Eq. (6). Then the remaining unknown kinetics parameters; i.e., K_2 and K_3, in Eq. (6) were continuously adjusted until the scatter best fitted a line that passes through the origin and makes a slope that equals to 1. This procedure allowed obtaining all kinetics parameters (K_1 through K_5) and the results are shown in Table I. With this procedure, the C curve for A356.2 alloy was generated as shown in Figure 7.

Table I. The kinetics parameters for A356.2 alloy.

K_1	K_2	K_3 (J/mol)	K_4 (K)	K_5 (J/mol)
-0.00501	6.70×10^{-17}	8,887	890.31	130,000[13]

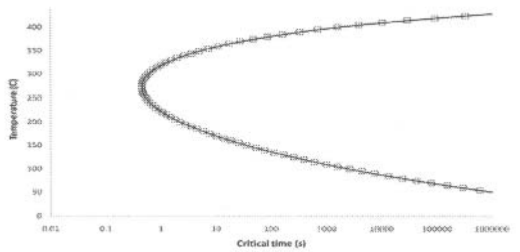

Figure 7. Generated C curve for A356.2 alloy.

Simulation results and comparison to measurements

The part shown in Figure 8 was designed, cast, machined, and equipped with two thermocouples as shown. Two different quenching processes were used to validate the model with this part. For both quenching processes, two identical parts were solutionized at 538°C (1000°F) for 12 hours and then one part was quenched into water that is maintained at 80°C (176°F) and the other part was air quenched by a stream of forced-air. For the water quench, the part was quenched by immersing the front face down into the water so that the blind cavity shown in Figure 8 (a) was filled with air as the part was quenched down to room temperature. For the forced air quench, the air was directly blown onto the front face of the part shown in Figure 8 (a). The time-temperature data was recorded from the two thermocouples. The part was then modeled as shown in Figure 9 and computer simulations were conducted with heat transfer coefficients assigned as follows:

For water quench: (1) the surface indicated by pink color in Figure 9 together with the face parallel to it were assigned the heat transfer coefficient that was measured by the quenching disk for hot water quenching, (2) the surfaces indicated by yellow color in Figure 9 were assigned the heat transfer coefficient measured for static air, and (3) all the other surfaces were assigned the heat transfer coefficient measured by the quenching probe for hot water quenching.

For air quench: (1) the face indicated by pink color in Figure 9 was assigned the heat transfer coefficient measured for air quenching, and (2) the other faces were assigned the heat transfer coefficient measured for static air.

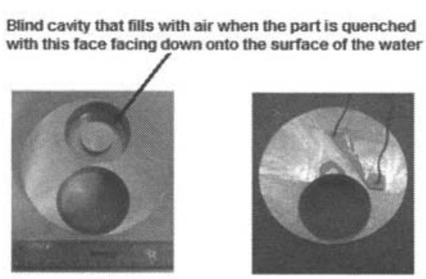

Figure 8. The part used for verification (a) front view, and (b) back view.

The computer-calculated cooling curves and cooling rates at the two nodes indicated by (1) and (2) in Figure 9 are reported. For the part quenched in hot water, the recorded and computer-calculated cooling data from the two locations are shown in Figure 10Figure 11. For the air quenched part, the results are shown in Figure 12. In all cases the results show excellent agreement between the measured and the computer-calculated cooling data indicating that the developed database of heat transfer coefficients and the method of locally assigning them to regions on a typical quenched part are accurate. Subsequently, two quenched parts were aged at 155°C (311°F) for 19 hours right after quenching, and HRB was measured on four different surfaces, as shown in Figure 13. The measured and computer-predicted hardness results are shown in Figure 14. In all locations, there is excellent agreement between the measured and the computer-predicted HRB values.

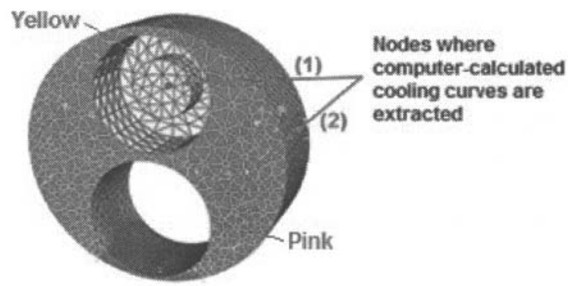

Figure 9. Modeling the part shown in Fig. 8.

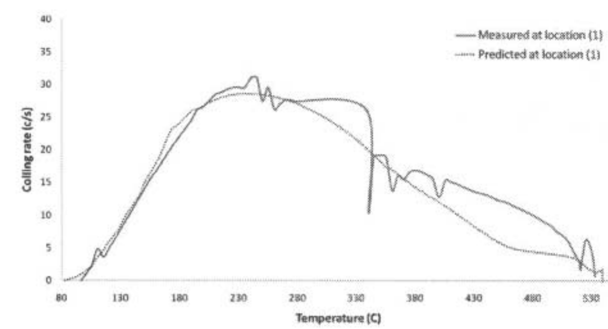

Figure 10. Measured and computer-calculated cooling curves at thermocouple location (1) for quenching in hot water.

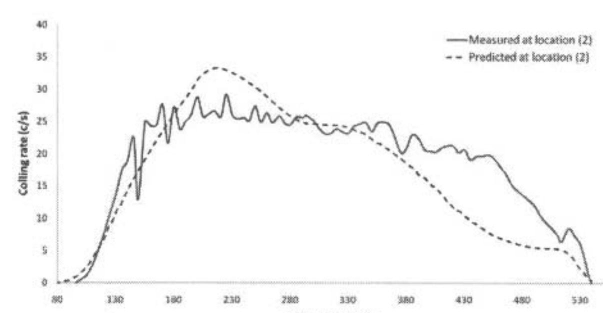

Figure 11. Measured and computer-calculated cooling curves at thermocouple location (2) for quenching in hot water.

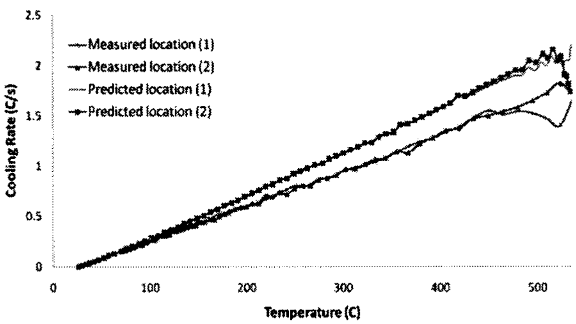

Figure 12. Measured and computer-calculated cooling rates at thermocouple locations (1) and (2) for quenching in air.

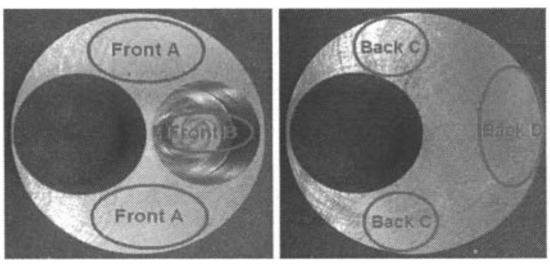

Figure 13. Indication of surface sections for hardness measurements.

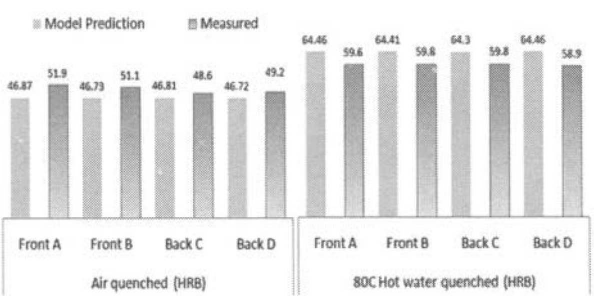

Figure 14. Measured and computer-predicted hardness for hot water quenched and air quenched parts.

Summary and Conclusions

A model has been developed using the ABAQUS finite element analysis software to predict the response of cast aluminum alloy components to solutionizing, quenching and aging processes. The necessary database for A356.2 alloy is generated. Both hot water and air quenching were selected for model validation. The thermal module within the model calculates the temperature profile for the quenching process using a database of temperature-dependant heat transfer coefficients and the new method of locally assigning them to regions on the quenched part. The user-developed property module which is based on a Quench Factor Analysis, predicts the local hardness values on the casting. The model predictions were verified by measurements made on heat treated parts, and the model-predicted cooling curves and hardness values were found to be in very good agreement with measured values.

References

1. J.W. Evancho and J.T. Staley,"Kinetics of precipitation in aluminum alloys during continuous cooling, " *Metall. Trans.*, 5 (1971), 43-47.

2. J.T. Staley, R.D. Doherty and A.P. Jaworski, "Improved model to predict properties of aluminum alloy products after continuous cooling," *Metall. Trans. A*, 24 (1993), 2417-2427.

3. J.T. Staley, "Quench Factor Analysis of Aluminum Alloys. Material Science and Technology," *Material Science and Technology*, 3 (1987), 923-935.

4. P.A Rometch, M.J. Starink and P.J. Gergson, "Improvements in quench factor modelling," *Mater. Sci. Eng*, A339 (2003), 255-264.

5. J.T. Staley and M. Tiryakioglu, "Use of TTP Curves and Quench Factor Analysis for Property Prediction in Aluminum Alloys, in Materials Solutions Conference" (Paper presented at Materials Solutions Conference, ASM International. Indianapolis, IN, 2001)

6. S.I. Bakhtiyarov, R.A. Overfelt, S.G. Teodorescu, "Electrical and thermal conductivity of A319 and A356 aluminum alloys," *Journal of Materials Science*, 36 (2001), 4643-4648.

7. M. Maniruzzaman, J.C. Chaves, C. McGee, S. Ma and R.D. Sisson, Jr., "CHTE Quench Probe System - a new quenchant characterization system, in the 5th International Conference on Frontiers of Design and Manufacturing" (Paper presented at the 5th International Conference on Frontiers of Design and Manufacturing, Dalian, China, 2002)

8. L.S. Tong and Y.S. Tang, *Boiling Heat Transfer and Two-Phase Flow* (CRC press 1997), 1-5.

9. R.G. Hills and E.C. Hensel Jr., "One-dimensional nonlinear inverse heat conduction technique," *Numerical Heat Transfer*, 10 (1956), 369-393.

10. K. Ho and R.D. Pehlke, "Metal-Mold interfacial heat transfer," *Metall. Trans. B*, 16 (1985), 585-594.

11. M. Li and J.E. Allison, "Determination of thermal boundary conditions for the casting and quenching process with the optimization tool OptCast," *Metall. Trans. B*, 38B (2007, 567-574.

12. M. Tiryakioglu and J. Campbell, "On macrohardness testing of Al-7wt.% Si-Mg alloys I. Geometrical and mechanical aspects," *Materials Scence and Engineering*, A361 (2003), 232-239.

13. R.J. Flynn and J.S. Robinson, "The application of advances in quench factor analysis property prediction to the heat treatment of 7010 aluminum alloy," *J. of Mater. Proc. Tech*, (2004), 674-680.

14. P.A. Rometch and G.B. Schaffer, "An age hardening model for Al-7Si-Mg casting alloys," *Materials Scence and Engineering*, A325 (2002), 424-434.